Soft Matter

Cite this: *Soft Matter*, 2012, **8**, 11589

www.rsc.org/softmatter

REVIEW

Smart electroresponsive droplets in microfluidics

Jinbo Wu,[a] Weijia Wen*[a] and Ping Sheng*[ab]

Received 4th June 2012, Accepted 26th August 2012
DOI: 10.1039/c2sm26286j

We give a short review of droplet microfluidics with the emphasis on "smart" droplets, which are based on materials that can be actively controlled and manipulated by external stimuli such as stress, temperature, pH, and electric field or magnetic field. In particular, the focus is on the generation and manipulation of droplets that are based on the giant electrorheological fluid (GERF). We elaborate on the preparation and characteristics of the GERF, the relevant microfluidics chip format, and the generation and control of droplets using GERF as either droplets or the carrier fluid. An important application of the GERF droplets, in the realization of first universal microfluidic logic device which can execute the 16 Boolean logic operations, is detailed.

I. Introduction

In the late 1980s, at the 5th International Conference on Solid-State Sensors and Actuators, Manz and collaborators advanced the concept[1] of 'total chemical analysis system (μTAS)' that emphasized the importance of microdevices in chemistry and bio-testing. Subsequently, this general concept has spawned a diverse field of investigation with descriptive terms such as 'microfluidics', 'bio-MEMS', 'lab-on-a-chip', *etc*. Microfluidics, in particular, relates to the new discipline involving the transport phenomena and fluid-based devices at the micron scale. In past decades, this area has undergone explosive development, serving as the common platform upon which engineers, physicists, chemists, biologists and others can interact and innovate on a vast array of research directions and applications that range from sensors, chemical/biological synthesis, microreactors, to drug discovery and point-of-care (POC) diagnostic.[1–3] Microfluidics technology has been employed in the development of inkjet print-heads,[4] lab-on-a-chip technology,[5] microthermal technologies,[6] *etc.* There is great promise that microfluidics would enable the integration of multiple steps of complex analytical procedures, micro- to nanoliter consumption of reagents/samples, as well as carrying out all the promised processes with portability.[7–9]

At present, microfluidics technology has two different approaches: continuous flow microfluidics and droplet microfluidics. Both have their own special characteristics and applications. Continuous flow microfluidics is more mature, droplet microfluidics is gaining recognition from its distinct micro-maneuverability and control.

Continuous-flow devices offer fine-tuned control of flow characteristics, its scaling up is a challenge as the size of devices

[a]*Department of Physics, The Hong Kong University of Science and Technology, Clear Water Bay, Kowloon, Hong Kong, China. E-mail: phwen@ust.hk*
[b]*Institute for Advanced Study, The Hong Kong University of Science and Technology, Clear Water Bay, Kowloon, Hong Kong, China. E-mail: sheng@ust.hk*

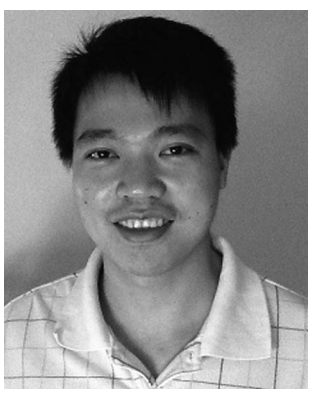

Jinbo Wu

Jinbo Wu's research interests are focused on droplet-based microfluidics, PCR biochip, and surface modification with patterning.

Weijia Wen

Weijia Wen's main research interests include soft condensed matter physics, electro-rheological (ER) and magneto-rheological (MR) fluids, field-induced pattern and structure transitions, micro- and nano-fluidic controlling, microsphere and nanoparticle fabrications, thin film physics, band gap materials, metamaterials and nonlinear optical materials.

increases almost linearly with the number of parallel channels. In contrast, droplet-based microfluidics, in which a large number of reactions can be run in parallel without having to increase the device size or complexity, has attracted more and more interest.[10] Chemical reactions and biological testing can be independently minitrarizied into tiny droplets ranging from nano- to picoliters in size. This can serve as a unique advantage of droplet-based microfluidics.[11,12] Below we further elaborate on this point.

In the form of droplets, reagents are conveyed precisely in discrete volumes that can act as vessels for reagents, thereby enabling single-cell manipulation in bio-testing[11,13,14] and high-throughput chemical reactions.[1,15] It provides a promising avenue for spatially and temporally resolved chemistry,[16] which can be used for inexpensive and potentially improved measurements of kinetic and binding constants, as well as measuring aspects of phase and reaction diagrams of multi-component systems.[16,17] Mixing of reagents in droplets has been proven to be achievable within milliseconds, hence multistep chemical reactions *via* droplet microfluidics has been shown to be possible.[18] Another advantage of droplet microfluidics is that the reagents/chemical/particles/cells in each droplet are well isolated, thus reducing contact with solid walls and potential contamination. The droplet microfluidic chip tends to be more multi-functional, with a simple and miniaturized structure. At present, droplet microfluidics is not only applied in DNA and protein analysis,[19–23] immunoassay[24] and chemistry,[25,26] but has also been found to be indispensable in some physical measurements,[27] droplet and bubble logic,[28] as well as clinical applications.[29,30]

Droplet microfluidics involves the generation, detection and manipulation of discrete droplets inside microdevices.[18,31] In what follows, we survey in Section II the approaches for generation and manipulation of droplets. In Section III the focus is on the "smart" droplets that are based on the giant electrorheological fluid (GERF). In particular, the preparation of the smart droplets, the relevant microfluidic chip design, and the maneuver and control of the smart droplets are detailed. Section IV presents an important application of the smart electro-responsive droplets in realizing the microfluidic logic gates that can eventually enable the self-sustaining operation of the microfluidic chips requiring minimal external control. We conclude in Section V with remarks regarding potential future developments.

Ping Sheng

Ping Sheng is the Dr William Mong Chair Professor of Nanoscience at the Hong Kong University of Science and Technology. His research interests are in the areas of complex fluids, hydrodynamic boundary conditions, electrorheological fluids, photonic and phononic wavefunctional materials, and carbon nanotube superconductivity.

II. Droplets generation and manipulation

2.1 Droplets generation

The special utility of droplet-based microfluidic systems lies in the formation of uniform droplets and particles. Intrinsic to such systems, and of utmost importance, is the precise control of the size, shape and monodispersity of the droplets. The microfluidic flow-focusing (MFF) method is often used in droplet/bubble formation,[32,33] the generation of double emulsions,[34–36] multi-functional particles and microbeads.[37] Weitz's group has developed novel, facile, and scalable techniques using glass capillary for producing single, double, and higher order monodisperse emulsions with exceptional precision. These emulsions are useful for a variety of applications ranging from microparticle fabrication (multilayers, multicore or non-spherical) to vesicle formation and chemical synthesis to high-throughput screening where each droplet serves to encapsulate single cells, genes, or reactants.[38–40]

Another geometry-based generation method uses the T-junction configuration, by which two immiscible fluids are brought together. Basic research into this method has been conducted by Quake's group,[41] Weitz's group[42] and others.[43] Many active generation control methods have been developed, such as aspiration,[44] external force,[45] acoustic wave,[46] electrolysis,[47] high-voltage pulses,[14] electrowetting[48] and thermocapillary.[49]

2.2 Droplets manipulation

Unlike continuous microfluidics, droplet microfluidic systems allow independent control of droplets, so that generated droplets can be individually split, mixed, transported and analyzed.[50] Droplet operations can include fission, fusion, sorting, mixing enhancement, and detection. Both the passive and active methods have been utilized in droplet manipulation.

2.2.1 Passive manipulation. Passive methods usually depend on the channel structure, either in 2D or 3D. Channels with branches or obstructions are designed to create a shear force for splitting droplets.[51–53] When a droplet is pushed to the bifurcating junction, the branches can pull on the droplet, causing it to break up into two, either symmetrically or asymmetrically. In these designs, droplet fission may be controlled by flow rates. Fusion of droplets is usually conducted by bringing two or more droplets close to each other until a thin film of fluid forms, connecting the interface.[54] Channel geometries designed for this purpose can include side channels to drain the continuous phase between the droplets.[51,55] Mixing within a droplet is another important issue for droplet microfluidics. In each half of a droplet that touches the channel wall, equal re-circulation flow can be generated. Thus fluids in each half of the droplet are well-mixed but the two halves remain separated from each other.[49] Passive droplets mixing is usually enhanced by a winding channel to fold, stretch and re-orient the droplets.[16,17] Passive droplet sorting often depends on the droplet size. Channel geometry and branches can be carefully designed to differentiate size differences.[56] Passive transport control of individual droplet is noted to still remain a challenge.

2.2.2 Active manipulation. Many active control methods have been realized, such as *via* hydrostatic pressure,[57] temperature gradient,[58] thermal expansion,[59] optical approaches,[60–62]

magnetic field[63] and electric-related approaches[13,64,65] that include electrostatic,[66] electrokinetic effect,[67] dielectrophoresis[68] and electrowetting.[48,69–73] Among them, electrowetting on dielectric (EWOD)[69,74,75] has been proven to be very effective for cutting, merging, creating and transporting liquid droplets. Such a type of technology has been denoted as digital microfluidics (DMF), so named because of its finely tuned "digital" control of droplets. All droplet manipulations—dispensing, moving, splitting and merging—are conducted by using EWOD to drive the droplet movement, with every single step defined by external control. In contrast, for the smart droplet logic gate described below, logic operations are carried out through interaction among the droplets, which greatly simplifies the control that is necessary for realizing the logic operations.

2.3 Smart droplets

Smart droplets are based on smart or intelligent materials that can respond to external stimuli such as stress, temperature, pH, and electric field or magnetic field.[76] Compared to the conventional droplets, the generation and manipulation of the smart droplet can be more easily controlled by external stimuli in an active manner.

To date, several kinds of smart (responsive) droplets have been reported and classified according to their response to external control. (1) Thermal responsive droplets. By incorporating TiO_2 nano particles[77] or other materials such as wax[78] into droplets, the surface tension or viscosity of the fluid droplets can be made to be temperature dependent. In particular, Seiffert *et al.* and Shah *et al.* have formed thermoresponsive smart microgel capsules from macromolecular precursors and demonstrated their utility for encapsulation and controlled-release applications.[79,80] (2) pH responsive droplets. Khan *et al.* fabricated smart emulsion coated with a pH-sensitive polymeric hydrogel whose surface charge property can be changed by external pH value.[81,82] (3) Photo responsive droplets. Matsumoto *et al.* successfully developed a photo-responsive gel droplets which can transform to the sol state under UV exposure.[83] (4) Magnetic responsive droplets such as ferrofluid droplets. Ferrofluid droplets can be actuated in a magnetic field, by changing its magnetic rheological properties.[84,85] It can also be used in the actuation of a pump or valve[86] and has been reviewed by Nguyen.[87] (5) Electric responsive droplets such as electrorheological fluid droplets. By employing the giant electrorheological fluid (GERF),[88] a series of fully chip-embedded soft-valves[89,90] and a fluidic-based automatic smart system have been realized. Below we focus on the GERF as the enabling material for the smart droplets. Compared to all the other smart droplets, the electro-responsive smart droplets offer the advantage of not only being "smart" on their own, but can also be used to control other types of droplets. This point will be further discussed in detail below.

Table 1 summaries, in pictorial form, the five types of smart droplets described above.

Electrorheological fluid (ERF) is a type of smart material comprising dielectric particles suspended in an insulating oil.[92] Owing to the contrast in the dielectric constant between the solid particles and the dispersing liquid, solid particles are polarized under an applied electric field, leading to an induced dipole moment (Fig. 1). The resulting dipole–dipole interaction and the energy minimization requirement dictate that the particles would aggregate to form columns along the applied field direction. This structural transformation, which can occur within a few milliseconds, causes the ER fluid to exhibit increased viscosity or even solid-like behavior, *i.e.*, the ability to sustain the shear stress[93–101] (Fig. 1). ERF can serve as an electrical–mechanical interface, and when coupled with sensors to trigger the timing and magnitude of the applied electric field, it can render many devices such as clutches, valves, dampers and others to become active mechanical elements capable of responding to environmental variations – hence the denotation of "smart" fluid. However, in spite of broad interest in the envisioned diverse applications, actual realization of these useful potential has been hampered by the inadequate ER effect exhibited by the traditional ERF. Considerable improvement efforts have gone into the preparation of alternative suspended particles,[102–104] but to no appreciable effect.

A breakthrough was achieved in 2003 (ref. 88) with the discovery of the giant electrorhelogical fluid (GERF), comprising urea-coated barium titanyl oxalate nanoparticles suspended in silicone oil. The GER effect represents a different paradigm from the conventional ER mechanism as it is based on molecular dipoles instead of induced dipoles. It offers a significantly higher

Table 1 Illustration of 5 types of smart droplets. (1) The droplet size decreases as the temperature increases.[84,85] (2) The droplet is positively charged at pH = 4 while it turns neutral at pH = 9.[91] (3) The shell of two droplets, under UV irradiation, turns into the sol state from the gel state, and the two droplets fuse into one.[83] (4) Magnetic particles suspended in a droplet form chains when a magnetic field is applied.[86] (5) Dielectric particles suspended in a droplet form chains when subjected to an electric field[92]

Smart droplets	Examples
(1) Thermal responsive droplets	
(2) pH responsive droplets	
(3) Photo responsive droplets	
(4) Magnetic resposive droplets	
(5) Electric responsive droplets	

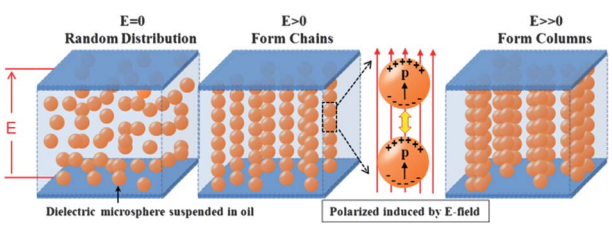

Fig. 1 The structural evolution of dielectric microspheres under an increasing electric field. From left to right: no field, a moderate field and a strong field.

ER effect.[88] Under a moderate electric field, GERF can transform into an anisotropic solid, with a yield stress on the order of 100–300 kPa at 4 kV mm^{-1} of the electric field. These rheological variations can occur within 10 milliseconds and are reversible when the field is removed. With such remarkable features, a range of device applications[88,105–108] as well as microfluidic microvalve, micropump, and highly maneuverable microplatforms *etc.*, have been realized.[89,90,109–112]

In what follows we detail the generation process of GERF droplets and the flow and droplet train manipulations that can be achieved. In conjunction with the use of the Ag–PDMS composite as conducting wires and the microfluidic channel as part of electrical circuit's capacitance/resistance, it is shown that logic functions can be realized on microfluidic chips, through the nonlinear electrical-flow response of the GERF droplets.

III. GERF-based smart droplets

3.1 GERF composition and characteristics

For the GERF to be used in the microfluidics context, it is necessary to avoid the absorption of silicone oil, the traditional suspending fluid for GERF, by the basic chip material PDMS. Hence for microfluidic applications the GER particles are suspended in sunflower oil instead, with a weight ratio of 5–40% GER particles. The mixture is filtered with sieves (with pore size around 10 mm) to remove the large aggregates.

Under an applied field >1 kV mm^{-1}, the GERF exhibits solid-like behavior, *e.g.*, the ability to transmit the shear stress. The measured dynamic shear stress of the sunflower oil-based GERF is comparable to that of the silicone oil-based GERF under similar electric fields. As the GERF has a much larger ER response under the same applied field (Fig. 2) compared with the traditional ERF, a moderate electric field is sufficient for slowing down or stopping the microfluidic flow, for both the droplet generation and manipulation processes. This is a crucial aspect that has enabled the development of GERF-based smart droplets in microfluidics.

3.2 Chip fabrication

To control the GERF droplets, electrodes have to be integrated into the PDMS microfluidic chips. However, metal does not adhere well to the PDMS, owing to its low surface energy. To overcome this problem, conductive particles such as carbon fibers/carbon black or Ag nanoparticles were embedded or added into PDMS, to form conducting composites that can be compatibly processed through soft lithography.[114,115] Two types of PDMS-based conducting composites (silver/carbon PDMS – Ag/C PDMS) have been developed by Niu *et al.*[116] These mixtures can be made into a thin film with desired thickness or patterned into structures and embedded in PDMS microfluidic chips by soft-lithography. Planar and 3D conducting microstructures, ranging from tens to hundreds of micrometers, have been successfully integrated into PDMS-based chips.

By using the PDMS conducting composites, pairs of parallel and channel-wall-embedded electrodes can be installed across the microfluidic channel. With the input electric signal, electrical control and sensing become achievable as part of GERF droplet control. In particular, very small variations in the capacitance can be detected when a droplet passes through between the two electrodes. Due to the electrodes' design and feedback electronic circuit, accurate real-time determination of size, shape and composition of droplets has been demonstrated (Fig. 3). The operational frequency can reach up to 10 kHz, a speed which is difficult to be realized by conventional optical means. Thus, it can be used in portable lab-chip for *in situ* detection and control of droplets. The tested capacitance signals can be used directly for *in situ* labeling, sorting and droplet manipulation.

3.3 GERF as droplets or as a carrier fluid

There are two ways of applying the GERF into the microfluidic channel for droplet manipulations. The first is to form GERF droplets carried by another fluid, while the second is to use GERF as the carrier fluid to control other liquid droplets or bubbles. A schematic of the two cases is shown in Fig. 4(a) and (b). The electrodes placed on the sides of microfluidic channels can apply the electric field to the flowing GERF, either in the form of droplets or as the carrier fluid. The electrodes at the droplet generation section of the chip are located near the junction area so as to control the timing of the GERF flow, thereby giving control to the generation of droplets. Downstream electrodes provide further flow control in the form of sensing, routing, and/or sorting.

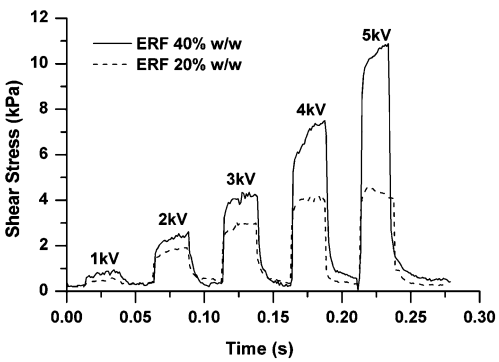

Fig. 2 Calibration of the ER effect for two sunflower oil-based GERF with nanoparticle concentrations of 20% and 40%. The dynamic shear stress is plotted as a function of time. 1 kV to 5 kV square wave DC voltage pulses were applied to the sample across a 1 mm gap.[113]

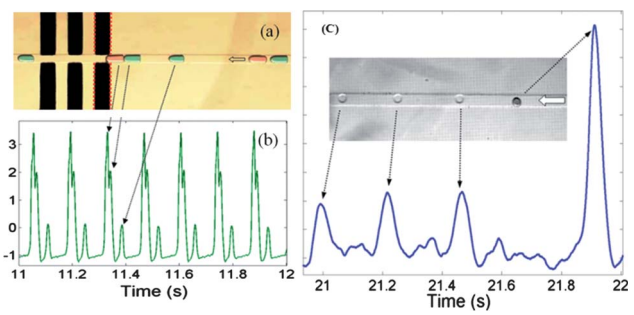

Fig. 3 (a) Optical image of a group of DI water droplets with different sizes. A small amount of dyes (without causing detectable variation of the dielectric constant for the droplets) was added for labeling. The detected signals are depicted in (b). (c) Detected signals with arrows pointing to the corresponding droplets: dyed DI water (dark) and ethylene glycol (light).[117]

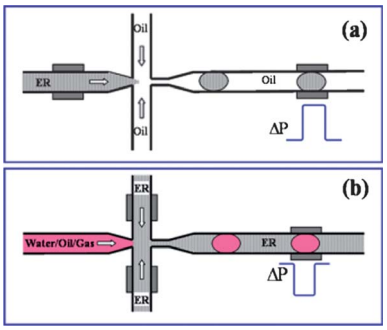

Fig. 4 Schematic view of the GERF as (a) droplets[113] and (b) the carrier fluid[118] in the microfluidic channels.

Below we review the two cases of GERF as droplets or as a carrier fluid, and their respective capabilities.

3.3.1 GERF smart droplet generation. In the first approach, GERF droplets are generated by the flow-focusing approach as shown schematically in Fig. 4(a). When the voltage on a pair of electrodes at the droplet generation section is set to zero, GERF droplets can be generated in a passive manner. Inset (b) of Fig. 5 shows mono-dispersed droplet generation when the flow rate of GERF is at 0.2 ml h^{-1} and the ratio of silicone oil (as the carrier fluid) to GERF flow is 3 : 1. However, when the flow rate is high (4 ml h^{-1}) and the oil ratio is increased to 10 : 1 (see inset (c)), the generated GERF droplets have a much higher poly-dispersity.

GERF droplets also can be generated in an active scheme by applying a square wave pulsed electric field signal on this pair of electrodes. Very uniform droplets—stable over a wider range of flow rates—are shown in Fig. 5(d, e). The period T of the electrical pulse is noted to be a critical parameter for stable GERF droplet production. In particular, instability sets in when T is beyond a certain working range that has been determined to range from 100 ms to 1000 ms, at a flow rate of GERF = 0.4 ml h^{-1}. By using two or more independent GERF inlets, both operating in the stable regime, GERF droplet synchronization and relative phase variation can be easily achieved. The generated droplet length is plotted as a function of T in Fig. 5(a) for four flow rates. Moreover, the electric signals need not be periodic. Arbitrary pulse trains can be used to generate GERF droplet chains with desired droplet size and distance. Two examples are shown in Fig. 5(f). In all cases droplet generation and the applied electric signal are well matched, *i.e.*, the GERF droplet chains are encoded by the electric signal. In the case of the thermal responsive smart material, Murshed *et al.* have demonstrated temperature dependence of nanofluid droplet size during the generation process,[77] while Seiffert *et al.* have shown that the droplet (microgel capsule) size can also vary as a function of temperature, from 60 μm to 120 μm after generation.[79]

3.3.2 Flow control with GERF smart droplets. Fig. 6 shows two types of GERF smart droplets generated with two different nanoparticle concentrations. The top three panels, Fig. 6(a)–(c) pertain to droplets with 40 wt% nanoparticles, whereas Fig. 6(d) is for GERF droplets with a lower percentage, 5 wt%, of nanoparticles. Fig. 6(a) shows a smart droplet with no electric field applied. It has a spherical shape. In Fig. 6(b), when an electric

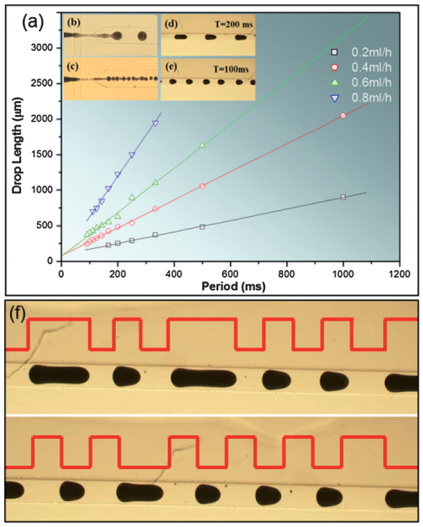

Fig. 5 (a) Smart droplet generation under different GERF flow rates, with droplet length (normalized by flow rate) plotted as a function of the period T of the electrical control signals.[113] (f) Optical microscopic images of two groups of GERF droplets generated by control electrical signals (red line).

field (1500 V mm^{-1}) is applied, the droplet is seen to be elongated with the two ends touching the electrodes. This would slow down or even stop the motion of this droplet. When the field is removed, the droplet resumed its original spherical shape and moved on again, as shown in Fig. 6(c). To observe the encapsulated GER particles more clearly, deformation of several smart droplets with a lower nanoparticle concentration is shown in Fig. 6(d). The droplet on the left is outside the influence of the electric field, and it has a spherical shape. But for those under an applied electric field, every droplet is stretched, accompanied by the clearly visible separation of the nanoparticles from the sunflower oil. In particular, the chains/columns formed by the nanoparticles are plainly identifiable, and the sunflower oil is seen to be pushed forward to form a curved front with the silicone oil, owing to the differential pressure generated by the slowed channel flow.

Fig. 6(e) shows the measured differential pressure $\Delta P = P_1 - P_2$ sustained by the GERF droplets at two different nanoparticle concentrations. It is seen that the increase in the differential pressure displays a nonlinear behavior, with saturation at a higher electric field strength that is different from the near-linear dependence of the dynamic shear stress. Detailed inspection of the second inset in Fig. 6(e) reveals that the particles have less density close to the channel wall than in the middle. However, the maximum differential pressure is more than 90 kPa mm^{-1} for the GERF fluid with 40 wt% nanoparticles. Such a differential pressure is adequate for most of the microfluidic applications.[119] The differential pressure induced by the smart droplets can be adjusted readily by varying the strength of the electric field, droplet size and nanoparticle concentration in the GERF.

3.3.3 Micro droplet display by GERF smart droplets. As both GERF droplet generation and flow can be controlled, a microfluidic chip with integrated function of droplet encoding, sorting, storage and other manipulations may be achieved. Shown in

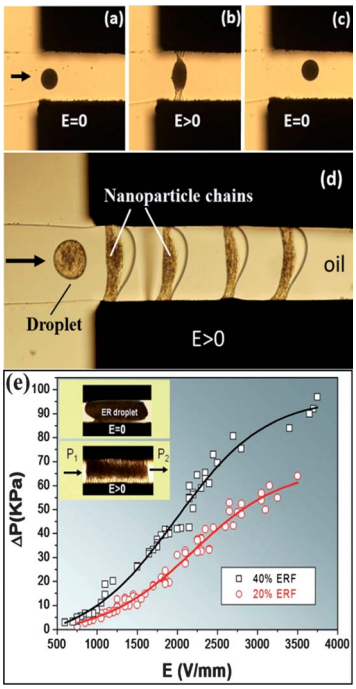

Fig. 6 (a)–(c) Optical images of a GERF droplet deformed by an applied electric field and restored when the field is removed. (d) A sequence of GERF particles under an applied electric field. Phase separation inside the GERF particle is clearly seen. (e) Differential pressure generated by the GERF droplets under different electric fields, for two different nanoparticle concentrations in the GERF.[113]

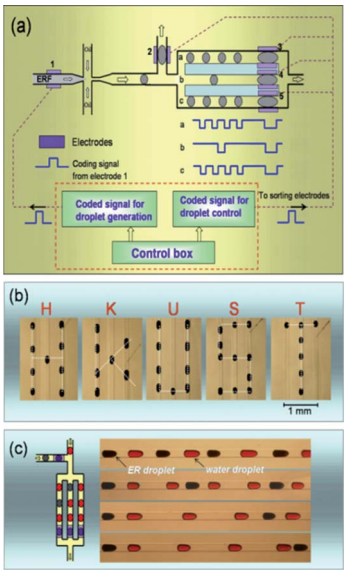

Fig. 7 (a) Flow chart and control circuit for the generation of a smart droplet display. (b) Optical images of the smart droplet display. (c) A sketch (left) of the chip component showing the orthogonal channels to form the water droplet "packages", and optical images (right) of the generated packages formed with different numbers of water (red) droplets sandwiched between two GERF smart (black) droplets.[113]

Fig. 7(a) is a schematic illustration of a designed chip to realize such functions. Three downstream channels are used to store the smart droplets so as to form a display panel with the desired characteristics. An example for displaying the character "H" is illustrated in Fig. 7(a). Fig. 7(b) shows the resulting display with the characters "HKUST" clearly visible.

By injecting smart droplets among the water droplet trains, "packages" of any desired number of water droplets can be sandwiched between two smart GERF droplets. Fig. 7(c) shows the schematic illustration for one part of such a chip (left) and some snapshots of the experimental results (right). The injection frequency and phase (relative to the water droplets) of the smart droplets are adjusted so that one smart droplet leads the train of water droplets.

In this context it should be noted that in a similar fashion but by using magnetic field control, Sun *et al.* have demonstrated that a small ferrofluid plug can be driven by an external magnet along a circular microchannel, for the purpose of circulating the polymer chain reaction (PCR) mixture through 3 temperature zones.[85]

By controlling the smart droplets, the train of water droplets can be directed, sorted and delivered to a targeted destination inside the chip, where mixing, heating and/or other processing may be carried out. All such controls can be digitally programmed.

3.3.4 Droplets generation with GERF as the carrier fluid. In the second approach, GERF is used as the carrier fluid. The droplet generation control is illustrated in Fig. 4(b). Similar to the first method, two pairs of electrodes located at the generation section of the chip are used to apply the electric signals to control the droplet generation. Any fluid, which is immiscible with the sunflower oil, can be converted into desired droplets by this method. Examples of the droplet fluid include oil, water or even gas. Dyed deionized water was used for demonstration. Fig. 8 shows the effect of the frequency of the applied electric signals at different injection rates for both the flow-focusing and T-junction droplet generation structures. The left upper insets of Fig. 8(a) and (b) are optical images of droplet profiles generated with the flow-focusing and T-junction structures, respectively. They have been carried out at a fixed flow rate without the electrical control signals. It should be noted that, without the application of control signals the water droplet size is determined by the relative flow rates between the GERF stream and the water stream. This is denoted as the passive droplets generation regime. On this basis, water droplets with tunable sizes may be obtained through the active control of the GERF stream.

As a function of applied electrical signals' frequency, a stable generation regime is found within which water droplet generation may be actively tuned by varying the frequency of the applied electric field. A one-to-one correspondence between the frequency of the applied control signal and the rate of droplet generation can be established. In Fig. 8, the stable droplet generation regime is delineated by the grey area in the frequency–flow rate map. For the flow-focusing structure, if the flow rates of water and GERF are both fixed at 0.1 ml h^{-1}, the generation rate of droplets may be varied from 7 to 17 droplets per second by tuning the electrical signal frequency. This is indicated by a dashed line in Fig. 8(a). From the optical images, one can observe that in the stable regime, uniform droplets train can be generated.

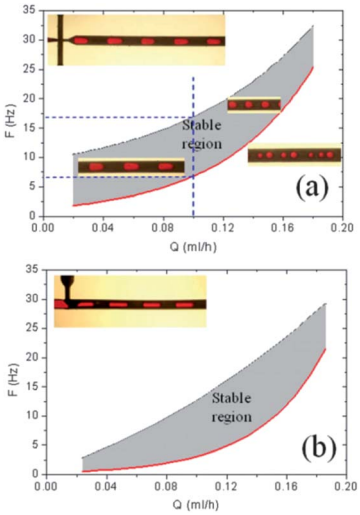

Fig. 8 Frequency of droplet generation using two different structures, plotted as a function of the flow rate Q. The stable region is denoted by grey.[118] The flow focusing geometry is shown in (a) and T-junction in (b). The dashed lines in (a) are intended to delineate the upper and lower bounds of the generation frequency for stable droplet generation, at $Q = 0.1$ ml h^{-1}.

Beyond the stable regime the droplets generation is characterized by irregularly spaced droplets of different sizes. From Fig. 8(a) and (b), we conclude that for both the flow-focusing and T-junction structures the droplet generation rate and the droplet size can be easily tuned by external electric signals. This is denoted as the active droplet generation approach.

By using a similar flow-focusing generation device as described above, the control of gas bubbles (such as N_2 bubbles) has also been demonstrated (Fig. 9 (a)–(c)).

It is observed that the droplet generation and the applied electric signal are well matched, and the bubble chain can be encoded by the electric signal. Alternatively, since the GERF is electrically controllable, the bubble generation can be digitally controlled by applied electric signals without changing the gas pressure. Bubble generation control is an interesting topic especially in digital microfluidics, and it is also very useful for the application in bio-systems. The manipulation of bubbles is generally much more difficult, owing to their different characteristics compared to the liquid droplets. Nevertheless, the bubble size, flow direction as well as separation distance between the bubbles can be easily controlled with this approach.

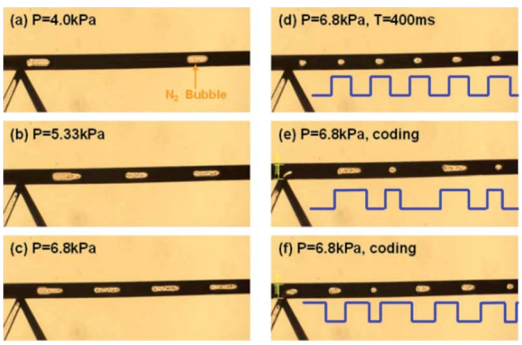

Fig. 9 (a–c) Optical images of N_2 bubbles generated under different gas pressures but at the same flow rate of the carrier fluid. No electrical control signal is applied. (d–f) Bubble generation under the same pressure and flow rate, but with different coded electrical signals (indicated by the blue solid lines).[118]

3.3.5 Multi-droplets manipulation and droplets order exchange. By using electrical signals and GERF, not only the droplets generation process, but also the phase of two or more types of the generated droplets, can be controlled. Fig. 10 shows two kinds of droplets generated in the same phase or opposite phase in the main channel. In Fig. 10(a), two types of droplets, dyed red and green, are generated with electrical pulsed signals that are in phase. Uniform pairs of droplets are seen. In Fig. 10(b) we show the same two types of droplets generated with control signals that are out of phase with each other. In this case there is no pairing. Also shown in Fig. 10(c) is the work of Link *et al.*,[120] who applied the electric field on the droplet generation process in order to induce droplet formation. The phase of the droplet break-off can be adjusted within the production cycle, accomplished by increasing the electric field above the critical break-off field only at the instant when the droplet is required.

Once generated, droplets can be encoded and stored, as described above. Here we illustrate the use of flow rate and directional control to switch the ordering(s) in a train of droplets. Consider a train of different droplets as a coded message. Switching the order of the droplets implies the ability to revise or correct the message.

The experimental setup and control mechanism are shown on the left panel of Fig. 11, where two droplets, the blue one (droplet A) and the orange one (droplet B) come into the main channel

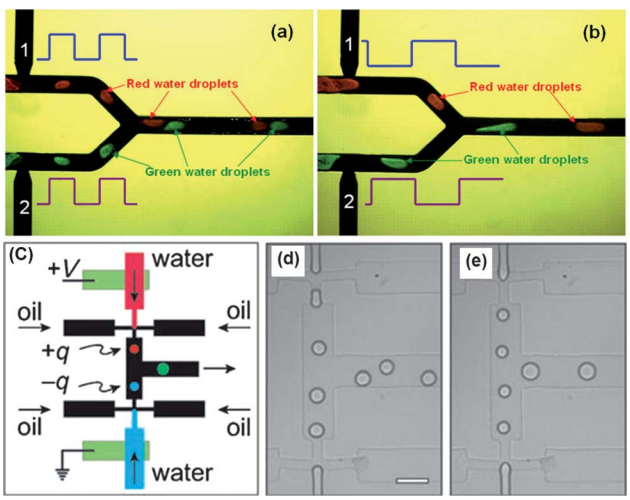

Fig. 10 (a–b) Controlled generation of two types of water droplets: (a) with the same phase of the control signals and (b) with the opposite phase of the control signals.[118] (c–e) Electrical control for two types of droplets generation.[120] (c) Droplets having opposite signs of electrostatic charge can be generated by applying a voltage across two aqueous streams. (d) The droplet is independently generated without an applied electric field. Each nozzle produces a different-sized droplet at a different frequency with same infusion rates at both nozzles. Droplets do not coalesce. (e) With an applied electric field, the droplets break off simultaneously from the two nozzles with the same phase. Droplets coalesce.

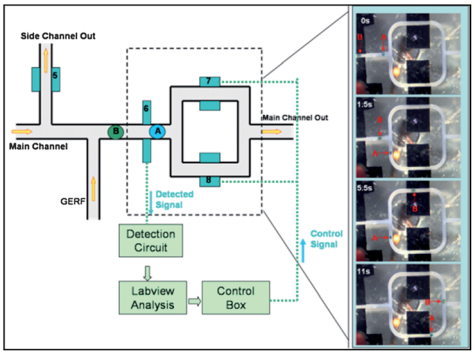

Fig. 11 Flow chart and control circuit for the droplet order exchange operation. The right insets are optical images taken at different times during the droplets exchange process.[118]

from the upstream, separated by a certain distance. By properly controlling the on–off duration of the applied voltages on electrodes 7 and 8, droplets A and B would resume their motion into the downstream with the ordering reversed. Thus ordering and separation distance between the droplets can be adjusted in accordance to one's demand. Such maneuverability may be very useful in droplet control for bio-systems and microfluidic computing.

IV. Microfluidic logic gate

The operation of complex microfluidic chips may eventually require extensive logic processes. While electronic logic gate can be extremely fast, to implement the logic operations on a microfluidic chip would require interfaces and additional controls. Microfluidic logic gate is envisioned to minimize external interfaces so as to enable the self-sustained execution of complex microfluidic operations.

To make the droplet control more automatic, the traditional electrical switch controlling the GERF's ON–OFF flow is supplemented by the conductive droplet/dielectric carrier fluid flowing in a nearby channel. The context of "inputs" is extended from the electric signal to droplet switches, *i.e.*, the sequence of droplets in the carrier fluid that can be sensed owing to the different dielectric constant or conductivity. To further elaborate on this point, we observe that as the designed electrodes are embedded on the sides of the microfluidic channels, the fluid channels (either the droplets or the carrier fluid) may be viewed as elements of the electric circuit, *i.e.*, as capacitance and/or resistance. When a droplet goes through a pair of electrodes, the electric properties between the electrodes will be changed, and the voltage is therefore re-distributed in the electrical circuit. These electrical signals can be used to trigger operations on the droplets of the nearby fluid channel. In this fashion, the smart droplets can 'communicate' with each other, and the logic operation can be carried out as a consequence. Furthermore, cascade connections and large-scale integration are possible.

4.1 Principle and device format

By definition, a logic gate is "an idealized or physical device implementing a Boolean function, that is, it performs a logical operation on one or more logic inputs and produces a single logic output."[121] For an input of 2 variables, there are 16 possible Boolean algebraic functions. A schematic illustration of a microfluidic logic gate is shown in Fig. 12(a). Here the GERF is denoted by the orange color, and green color denotes the signal electrolytic droplet fluid, which is conducting. The insulating carrier fluid is denoted by the light yellow color. The conducting Ag–PDMS composite is shown in grey. The fluid channels and pads are electrically connected *via* the conducting strips. With two parallel capacitances (top, near pads 1 and 2), the voltage on the output GERF channel, $|V_A - V_B|$, can be manipulated under different input combinations of V_1, V_2, V_3, and V_4. Since the flow of GERF can be stopped by a voltage $|V_A - V_B|$ that exceeds a threshold value V_C, this nonlinear characteristic serves as the enabling element for all the logic gate operations.

To effectively control the voltage on the GERF output channel, we have purposely made the parallel capacitances of the input signal GERF channels to have the same width and electrode sizes as the output control GERF channel. Thus the impedances of all three GERF channels are the same and equal to a constant Z_E. Therefore if the green (conducting) signal droplets are absent in the gap regions of channels *A* and *B*, then V_1 and V_2 would have very little effect on V_A or V_B since they are separated by the insulating (yellow) carrier fluid. In that case V_3 and V_4 control the value of $|V_A - V_B|$.

The situation changes when there is a (green) signal droplet in either gap A or gap B. When that happens, the conducting signal droplet would make the applied voltage V_1 or V_2 to be the same as V_A or V_B, respectively.

For the configuration as shown in Fig. 12(a), the voltage on the control GERF (central channel) can be expressed in general as

$$V_{GERF} = |V_A - V_B| = f(V_1, V_2, V_3, V_4, Z_A(X_A), Z_B(X_B)), \quad (1)$$

where V_A and V_B are the electric potentials on either sides of the output GERF channel; V_1 to V_4 are the voltages applied to pads 5, 6, 1, 2, respectively; $Z_A(X_A)$ and $Z_B(X_B)$ are the impedances provided by the signal channels A and B, respectively. Here $X_i = 1$ (i = A or i = B) indicates that a (green) signal droplet is present between the signal electrodes, and $X_i = 0$ indicates that only the carrier fluid is present between the electrodes.

As an example, if the signals are carried by the KCl droplets in silicone oil, the conductive KCl droplets serve as the trigger signals/switches ($R_{KCl} \sim 0\ \Omega$ and $R_{oil} \sim \infty$). In this particular case, voltage on the GERF output channel (central channel) should be

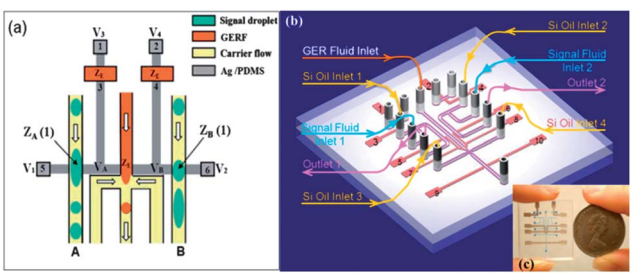

Fig. 12 (a) Schematic illustration of a logic gate. (b) Cartoon of universal logic gate's implementation. (c) Optical image of the universal logic gate chip with all the channels are filled with blue-dyed DI water for better visualization.[122]

$$V_{GERF} = f(X_A, X_B) = \begin{cases} f(0,0) = \frac{1}{3}|V_4 - V_3| \\ f(0,1) = \frac{1}{2}|V_3 - V_2| \\ f(1,0) = \frac{1}{2}|V_4 - V_1| \\ f(1,1) = \frac{1}{2}|V_1 - V_2| \end{cases} . \quad (2)$$

Assuming V_C to be the critical value required for GERF solidification, we can set a V_0 such that $2/3V_C > V_0 \geq 1/2V_C$, and the corresponding input voltage combination for 16 possible logic functions can be generated.

4.2 Universal logic with 16 Boolean logic operations

The implementation configuration of the microfluidic universal logic gate is shown in Fig. 12(b). The experimental testing results, as expected, show that all of the 16 Boolean logic operations can be effectively executed in this microfluidic chip,[122] the size of which is compared with that of a coin (Fig. 12(c)). This is the first microfluidic universal logic device in which all 16 Boolean logic operations (according to two inputs) can be realized. As there are 4 combinations of input signals (droplet status presented in the electrodes) from the A and B channels, [(X_A, X_B)= (0, 0), (0, 1), (1, 0) and (1, 1)] for each logic operation, there can be a total of 64 experimental results. Four logic operations can be merged into their mirrored ones (such as A → B into B → A and IF B into IF A), thus there are 48 independent configurations in total.

GERF droplets in this device are noted to serve not only as the fluidic logic output, but also as part of the electrical circuit and, most importantly, as a nonlinear electro-mechanical element for fluidic control. An output GERF droplet can be further utilized to provide the mechanical actuating/braking function, or for controlling/generating a third stream of signal fluid.

The GERF-based microfluidic logic chips have chip-embedded electrodes that can serve as data-exchanging interfaces with external devices such as oscilloscopes or PCs, thereby promising easy reprogramming and seamless integration with other devices. A real microfluidic droplet processor should resemble a CPU that can be "smart" enough to "think" by themselves,[28] with outputs fully dependent on inputs in assigned tasks. However, unlike electronic devices, traditional integrated microfluidic circuits are constrained by the fabrication process because they are designed within pre-shaped architectures for given tasks, with a lack of reprogrammability or cascadability.[123] In the present smart GERF droplet system, all functions of the universal logic gate can be realized in one fluidic configuration, requiring only the adjustment of voltage inputs, and these logic functions can be further coupled to complex tasks with ease.

V. Concluding remarks

We have given a short review of smart droplet microfluidics, with the focus on the electroresponsive smart droplets. In particular, GERF, comprising dielectric GER nanoparticles suspended in sunflower oil, is shown to be a versatile nonlinear electrical–mechanical interface in microfluidics. By being able to induce high differential pressure under applied voltage, GERF enables the control and manipulation of droplets in microfluidics. By using the GERF as part of the electrical circuit, logic functions may be realized through electric communication with neighboring microfluidic channels. As this logic gate has a universal structure for all the logic operations, its large-scale integration requires only structural repetition of identical units. System reprogramming, similarly, requires only the rearrangement of voltage inputs. The generated GERF droplets can be used either as an indicator of the chronological order of the signal droplets, or as the control of downstream manipulation, such as the merge of droplets for chemical reactions. Meanwhile, the aforementioned GERF-actuated microfluidic valve, mixer, pump, storage, display, droplet phase modulator and logic gate functionalities are all compatible with each other. Combined with these functions in microfluidic chips, multi-step reactions and biological testing in microfluidic chips may be achieved with minimal external control.

Notes and references

1 A. Manz, N. Graber and H. M. Widmer, *Sens. Actuators B*, 1990, **1**, 244–248.
2 P. S. Dittrich and A. Manz, *Nat. Rev. Drug Discovery*, 2006, **5**, 210–218.
3 V. Linder, *Analyst*, 2007, **132**, 1186–1192.
4 H. Seitz and J. Heinz, *J. Micromech. Microeng.*, 2004, **14**, 1140–1147.
5 D. J. Harrison, K. Fluri, K. Seiler, Z. Fan, C. S. Effenhauser and A. Manz, *Science*, 1993, **261**, 895–897.
6 M. K. Jensen, Y. Peles, A. Koşar and C.-J. Kuo, *Microfluid. Nanofluid.*, 2006, **2**, 387–397.
7 P. Fortina, S. Surrey and L. J. Kricka, *Trends Mol. Med.*, 2002, **8**, 264–266.
8 K. K. Jain, *Cambridge Healthtech Inst. Third Annu. Conf. Lab-on-a-chip and Microarrays*, 2001, 2, pp. 73–77.
9 L. J. Kricka, *Clin. Chim. Acta*, 2001, **307**, 219–223.
10 S.-Y. Teh, R. Lin, L.-H. Hung and A. P. Lee, *Lab Chip*, 2008, **8**, 198–220.
11 J. Clausell-Tormos, D. Lieber, J.-C. Baret, A. El-Harrak, O. J. Miller, L. Frenz, J. Blouwolff, K. J. Humphry, S. Köster, H. Duan, C. Holtze, D. A. Weitz, A. D. Griffiths and C. A. Merten, *Chem. Biol.*, 2008, **15**, 427–437.
12 W. Shi, J. Qin, N. Ye and B. Lin, *Lab Chip*, 2008, **8**, 1432–1435.
13 M. Chabert and J.-L. Viovy, *Proc. Natl. Acad. Sci. U. S. A.*, 2008, **105**, 3191–3196.
14 M. He, J. S. Edgar, G. D. M. Jeffries, R. M. Lorenz, J. P. Shelby and D. T. Chiu, *Anal. Chem.*, 2005, **77**, 1539–1544.
15 M. M. Kiss, L. Ortoleva-Donnelly, N. Reginald Beer, J. Warner, C. G. Bailey, B. W. Colston, J. M. Rothberg, D. R. Link and J. H. Leamon, *Anal. Chem.*, 2008, **80**, 8975–8981.
16 H. Song, J. D. Tice and R. F. Ismagilov, *Angew. Chem., Int. Ed.*, 2003, **42**, 768–772.
17 M. R. Bringer, C. J. Gerdts, H. Song, J. D. Tice and R. F. Ismagilov, *Philos. Trans. R. Soc., A*, 2004, **362**, 1087–1104.
18 S. L. Anna, N. Bontoux and H. A. Stone, *Appl. Phys. Lett.*, 2003, **82**, 364–366.
19 M. A. Burns, B. N. Johnson, S. N. Brahmasandra, K. Handique, J. R. Webster, M. Krishnan, T. S. Sammarco, P. M. Man, D. Jones, D. Heldsinger, C. H. Mastrangelo and D. T. Burke, *Science*, 1998, **282**, 484–487.
20 A. Huebner, M. Srisa-Art, D. Holt, C. Abell, F. Hollfelder, A. J. DeMello and J. B. Edel, *Chem. Commun.*, 2007, 1218–1220.
21 B. Zheng, J. D. Tice, L. S. Roach and R. F. Ismagilov, *Angew. Chem., Int. Ed.*, 2004, **43**, 2508–2511.
22 B. Zheng, J. D. Tice and R. F. Ismagilov, *Anal. Chem.*, 2004, **76**, 4977–4982.
23 B. Zheng, L. S. Roach and R. F. Ismagilov, *J. Am. Chem. Soc.*, 2003, **125**, 11170–11171.
24 V. Linder, S. K. Sia and G. M. Whitesides, *Anal. Chem.*, 2005, **77**, 64–71.
25 A. Imhof and D. J. Pine, *Nature*, 1997, **389**, 948–951.

26 I. Shestopalov, J. D. Tice and R. F. Ismagilov, *Lab Chip*, 2004, **4**, 316–321.
27 N.-N. Nguyen, S. Lassemono, F. A. Chollet and C. Yang, *IEE Proc.: Nanobiotechnol.*, 2006, **153**, 102–106.
28 I. R. Epstein, *Science*, 2007, **315**, 775–776.
29 V. Srinivasan, V. K. Pamula and R. B. Fair, *Lab Chip*, 2004, **4**, 310–315.
30 A. J. Tüdos, G. A. J. Besselink and R. B. M. Schasfoort, *Lab Chip*, 2001, **1**, 83–95.
31 D. Belder, *Angew. Chem., Int. Ed.*, 2005, **44**, 3521–3522.
32 K. Jensen and A. Lee, *Lab Chip*, 2004, **4**, 31N–32N.
33 P. Garstecki, A. M. Gañán-Calvo and G. M. Whitesides, *Bull. Pol. Acad. Sci.: Tech. Sci.*, 2005, **53**, 361–372.
34 S. Peng, M. Zhang, X. Niu, W. Wen, P. Sheng, Z. Liu and J. Shi, *Appl. Phys. Lett.*, 2008, **92**, 012108.
35 Z. Nie, S. Xu, M. Seo, P. C. Lewis and E. Kumacheva, *J. Am. Chem. Soc.*, 2005, **127**, 8058–8063.
36 H. C. Shum, J. Varnell and D. A. Weitz, *Biomicrofluidics*, 2012, **6**, 012808.
37 T. Nisisako, T. Torii and T. Higuchi, *Chem. Eng. J.*, 2004, **101**, 23–29.
38 R. K. Shah, H. C. Shum, A. C. Rowat, D. Lee, J. J. Agresti, A. S. Utada, L.-Y. Chu, J.-W. Kim, A. Fernandez-Nieves, C. J. Martinez and D. A. Weitz, *Mater. Today*, 2008, **11**, 18–27.
39 A. R. Abate and D. A. Weitz, *Small*, 2009, **5**, 2030–2032.
40 J. J. Agresti, E. Antipov, A. R. Abate, K. Ahn, A. C. Rowat, J.-C. Baret, M. Marquez, A. M. Klibanov, A. D. Griffiths and D. A. Weitz, *Proc. Natl. Acad. Sci. U. S. A.*, 2010, **107**, 4004–4009.
41 T. Thorsen, R. W. Roberts, F. H. Arnold and S. R. Quake, *Phys. Rev. Lett.*, 2001, **86**, 4163–4166.
42 A. R. Abate, A. Poitzsch, Y. Hwang, J. Lee, J. Czerwinska and D. A. Weitz, *Phys. Rev. E: Stat., Nonlinear, Soft Matter Phys.*, 2009, **80**, 026310.
43 T. Nisisako, T. Torii and T. Higuchi, *Lab Chip*, 2002, **2**, 24–26.
44 R. R. Pompano, W. Liu, W. Du and R. F. Ismagilov, *Annu. Rev. Anal. Chem.*, 2011, **4**, 59–81.
45 H. Willaime, V. Barbier, L. Kloul, S. Maine and P. Tabeling, *Phys. Rev. Lett.*, 2006, **96**, 054501.
46 U. Demirci and G. Montesano, *Lab Chip*, 2007, **7**, 1139–1145.
47 W. Olthuis, A. Volanschi and P. Bergveld, *Sens. Actuators, B*, 1998, **49**, 126–132.
48 S. K. Cho, H. Moon and C.-J. Kim, *J. Microelectromech. Syst.*, 2003, **12**, 70–80.
49 K. Handique and M. A. Burns, *J. Micromech. Microeng.*, 2001, **11**, 548–554.
50 R. B. Fair, *Microfluid. Nanofluid.*, 2007, **3**, 245–281.
51 Y.-C. Tan, J. S. Fisher, A. I. Lee, V. Cristini and A. P. Lee, *Lab Chip*, 2004, **4**, 292–298.
52 L. Ménétrier-Deremble and P. Tabeling, *Phys. Rev. E: Stat., Nonlinear, Soft Matter Phys.*, 2006, **74**, 035303.
53 D. R. Link, S. I. Anna, D. A. Weitz and H. A. Stone, *Phys. Rev. Lett.*, 2004, **92**, 545031–545034.
54 Y.-C. Tan, Y. L. Ho and A. P. Lee, *Microfluid. Nanofluid.*, 2007, **3**, 495–499.
55 X. Niu, S. Gulati, J. B. Edel and A. J. Demello, *Lab Chip*, 2008, **8**, 1837–1841.
56 Y.-C. Tan, Y. L. Ho and A. P. Lee, *Microfluid. Nanofluid.*, 2008, **4**, 343–348.
57 Y. Luo, Q. Zhang, J. Qin and B. Lin, *Electrophoresis*, 2007, **28**, 4769–4771.
58 A. Mazouchi and G. M. Homsy, *Phys. Fluids*, 2001, **13**, 1594–1600.
59 X.-S. Zhu, C. Gao, J.-W. Choi, P. L. Bishop and C. H. Ahn, *Lab Chip*, 2005, **5**, 212–217.
60 C. N. Baroud, M. Robert De Saint Vincent and J. P.- Delville, *Lab Chip*, 2007, **7**, 1029–1033.
61 G. D. M. Jeffries, J. S. Kuo and D. T. Chiu, *Angew. Chem., Int. Ed.*, 2007, **46**, 1326–1328.
62 D. Psaltis, S. R. Quake and C. Yang, *Nature*, 2006, **442**, 381–386.
63 J. Joung, J. Shen and P. Grodzinski, *IEEE Trans. Magn.*, 2000, **36**, 2012–2014.
64 C. Priest, S. Herminghaus and R. Seemann, *Appl. Phys. Lett.*, 2006, **89**, 134101.
65 K. Ahn, J. Agresti, H. Chong, M. Marquez and D. A. Weitz, *Appl. Phys. Lett.*, 2006, **88**, 264105.
66 D. R. Link, E. Grasland-Mongrain, A. Duri, F. Sarrazin, Z. Cheng, G. Cristobal, M. Marquez and D. A. Weitz, *Angew. Chem., Int. Ed.*, 2006, **45**, 2556–2560.
67 P. Carreras, S. Mohr, P. Fielden and N. Goddard, *Dig. Pap. - Microprocesses Nanotechnology; Int. Microprocesses Nanotechnology Conf.*, MNC, 2007, pp. 328–329.
68 J. A. Schwartz, J. V. Vykoukal and P. R. C. Gascoyne, *Lab Chip*, 2004, **4**, 11–17.
69 M. G. Pollack, A. D. Shenderov and R. B. Fair, *Lab Chip*, 2002, **2**, 96–101.
70 H. Ren, V. Srinivasan, M. G. Pollack and R. Fair, *Proc. MicroTAS.*, 2003, **2003**, 993–996.
71 P. Paik, V. K. Pamula, M. G. Pollack and R. B. Fair, *Lab Chip*, 2003, **3**, 28–33.
72 P. Paik, V. K. Pamula and R. B. Fair, *Lab Chip*, 2003, **3**, 253–259.
73 T. Taniguchi, T. Torii and T. Higuchi, *Lab Chip*, 2002, **2**, 19–23.
74 J. Lee, H. Moon, J. Fowler, T. Schoellhammer and C.-J. Kim, *Sens. Actuators, A*, 2002, **95**, 259–268.
75 S. K. Cho and H. Moon, *Biochem. J.*, 2009, **2**, 79–96.
76 T. Takagil, *J. Intell. Mater. Syst. Struct.*, 1990, 149.
77 S. M. S. Murshed, S.-H. Tan and N.-T. Nguyen, *J. Phys. D*, 2008, **41**, 085502.
78 R. Pal and M. A. Burns, *J. Micromech. Microeng.*, 2006, **16**, 786–793.
79 S. Seiffert, J. Thiele, A. R. Abate and D. A. Weitz, *J. Am. Chem. Soc.*, 2010, **132**, 6606–6609.
80 R. K. Shah, J. Kim and D. A. Weitz, *Langmuir*, 2010, **26**, 1561–1565.
81 W. Khan, J. H. Choi, G. M. Kim and S. Park, *Lab Chip*, 2011, **11**, 3493–3498.
82 W. C. Bauer, J. Kotar, P. Cicuta, R. T. Woodward, J. V. M. Weaver and W. T. S. Huck, *Soft Matter*, 2011, **7**, 4214–4220.
83 S. Matsumoto, S. Yamaguchi, A. Wada, T. Matsui, M. Ikeda and I. Hamachi, *Chem. Commun.*, 2008, 1545–1547.
84 N.-T. Nguyen, K. M. Ng and X. Huang, *Appl. Phys. Lett.*, 2006, **89**, 052509.
85 Y. Sun, Y. C. Kwok and N. T. Nguyen, *Lab Chip*, 2007, **7**, 1012–1017.
86 H. Hartshorne, C. Backhouse and W. Lee, *Sens. Actuators, B*, 2004, **99**, 592–600.
87 N.-T. Nguyen, *Microfluid. Nanofluid.*, 2012, **12**, 1–16.
88 W. Wen, X. Huang, S. Yang, K. Lu and P. Sheng, *Nat. Mater.*, 2003, **2**, 727–730.
89 X. Niu, W. Wen and Y.-K. Lee, *Appl. Phys. Lett.*, 2005, **87**, 1–3.
90 X. Niu, Y.-K. Lee, L. Liu and W. Wen, *Proc. IEEE Int. Conf. Nanol Micro Eng. Mol. Syst., IEEE-NEMS*, 2006, 1254–1257.
91 T. Liu, S. Seiffert, J. Thiele, A. R. Abate, D. A. Weitz and W. Richtering, *Proc. Natl. Acad. Sci. U. S. A.*, 2012, **109**, 384–389.
92 P. Sheng and W. Wen, *Annu. Rev. Fluid Mech.*, 2011, **44**, 143–174.
93 R. Tao and J. M. Sun, *Phys. Rev. Lett.*, 1991, **67**, 398–401.
94 D. J. Klingenberg, F. Van Swol and C. F. Zukoski, *J. Chem. Phys.*, 1989, **91**, 7888–7895.
95 K. C. Hass, *Phys. Rev. E: Stat. Phys., Plasmas, Fluids, Relat. Interdiscip. Top.*, 1993, **47**, 3362–3373.
96 L. C. Davis, *Appl. Phys. Lett.*, 1992, **60**, 319–321.
97 L. C. Davis, *J. Appl. Phys.*, 1992, **72**, 1334–1340.
98 H. Ma, W. Wen, W. Y. Tam and P. Sheng, *Phys. Rev. Lett.*, 1996, **77**, 2499–2502.
99 W. Y. Tam, G. H. Yi, W. Wen, H. Ma, M. M. T. Loy and P. Sheng, *Phys. Rev. Lett.*, 1997, **78**, 2987–2990.
100 T.-J. Chen, R. N. Zitter and R. Tao, *Phys. Rev. Lett.*, 1992, **68**, 2555–2558.
101 Y. Chen, A. F. Sprecher and H. Conrad, *J. Appl. Phys.*, 1991, **70**, 6796–6803.
102 B. H. Sung, Y. G. Ko and U. S. Choi, *Colloids Surf., A*, 2007, **292**, 217–223.
103 A. Krztoń-Maziopa, H. Wyciślik and J. Pocharski, *J. Rheol.*, 2005, **49**, 1177–1192.
104 I. S. Sim, J. W. Kim, H. J. Choi, C. A. Kim and M. S. Jhon, *Chem. Mater.*, 2001, **13**, 1243–1247.
105 W. Wen, X. Huang and P. Sheng, *Appl. Phys. Lett.*, 2004, **85**, 299–301.
106 C. Shen, W. Wen, S. Yang and P. Sheng, *J. Appl. Phys.*, 2006, **99**, 106104–106106.
107 X. Huang, W. Wen, S. Yang and P. Sheng, *Solid State Commun.*, 2006, **139**, 581–588.

108 X. Gong, J. Wu, X. Huang, W. Wen and P. Sheng, *Nanotechnology*, 2008, **19**, 165602.
109 X. Niu, L. Liu, W. Wen and P. Sheng, *Appl. Phys. Lett.*, 2006, **88**, 153508–153510.
110 X. Niu, L. Liu, W. Wen and P. Sheng, *Phys. Rev. Lett.*, 2006, **97**, 044501.
111 L. Liu, X. Niu, W. Wen and P. Sheng, *Appl. Phys. Lett.*, 2006, **88**, 173505–173507.
112 L. Liu, W. Cao, J. Wu, W. Wen, D. C. Chang and P. Sheng, *Biomicrofluidics*, 2008, **2**, 034103.
113 X. Niu, M. Zhang, J. Wu, W. Wen and P. Sheng, *Soft Matter*, 2009, **5**, 576–581.
114 S.-P. Rwei, F.-H. Ku and K.-C. Cheng, *Colloid Polym. Sci.*, 2002, **280**, 1110–1115.
115 A. J. Gawron, R. Scott Martin and S. M. Lunte, *Electrophoresis*, 2001, **22**, 235–241.
116 X. Niu, S. Peng, L. Liu, W. Wen and P. Sheng, *Adv. Mater.*, 2007, **19**, 2682–2686.
117 X. Niu, M. Zhang, S. Peng, W. Wen and P. Sheng, *Biomicrofluidics*, 2007, **1**, 044101–044112.
118 M. Zhang, J. Wu, X. Niu, W. Wen and P. Sheng, *Phys. Rev. E: Stat., Nonlinear, Soft Matter Phys.*, 2008, **78**, 066305.
119 M. A. Unger, H.-P. Chou, T. Thorsen, A. Scherer and S. R. Quake, *Science*, 2000, **288**, 113–116.
120 D. Link, E. Grasland-Mongrain, A. Duri, F. Sarrazin, Z. Cheng, G. Cristobal, M. Marquez and D. Weitz, *Angew. Chem., Int. Ed.*, 2006, **45**, 2556–2560.
121 R. Jaeger, *Microelectronic Circuit Design*, McGraw-Hill, 1997.
122 M. Zhang, L. Wang, X. Wang, J. Wu, J. Li, X. Gong, J. Qin, W. Li and W. Wen, *Soft Matter*, 2011, **7**, 7493–7497.
123 L. Wang, X. Gong and W. Wen, *Top. Curr. Chem.*, 2011, **304**, 91–115.